

Through-space communication in a TTF–C₆₀–TTF triad†

Frédéric Oswald,^a Stéphanie Chopin,^b Pilar de la Cruz,^a Jesús Orduna,^c Javier Garín,^c Atula S. D. Sandanayaka,^d Yasuyuki Araki,^d Osamu Ito,*^d Juan Luis Delgado,^a Jack Cousseau*^b and Fernando Langa*^a

Received (in Montpellier, France) 18th September 2006, Accepted 27th November 2006

First published as an Advance Article on the web 19th December 2006

DOI: 10.1039/b613466a

A 2-pyrazolino[60]fullerene-based triad, possessing two TTF units connected with flexible long linkages, has been prepared. Fluorescence quenching was observed in polar and non-polar solvents, suggesting the existence of a through-space photoinduced charge separation process with rates faster than $3.8 \times 10^9 \text{ s}^{-1}$ and with high efficiency (>0.85). The charge separated states were confirmed by transient absorption spectra in the visible and near-IR regions. The longest lifetime of the charge separated state was found to be 230 ns in CH₂Cl₂ solvent.

Introduction

Covalently-linked ensembles of electron donor and electron acceptor moieties constitute a topic of great interest. Such ensemble systems represent good models for the study of photoinduced charge separation processes characteristic of photosynthesis,¹ and many of them have already been involved in the fabrication of photovoltaic devices.² In particular, in the search for the achievement of a quite long lifetime for the final charge separated state, and for enhancing the potential of corresponding donor–acceptor covalent assemblies towards practical applications under light illumination, syntheses of triads, tetrads and polyads have been reported. However, long sequences of reactions are usually necessary to synthesize such molecular systems.³ Furthermore, from these previous studies, obtaining sufficiently long-persisting, charge separated radical ion pairs appears to be difficult for simple molecular systems.

On the other hand, fullerene derivatives have been incorporated into many molecular systems that act as artificial reaction photosynthetic models due to their electrochemical and photophysical properties. Recently, it has been revealed that tetrathiafulvalene (TTF) derivatives, which are well known as excellent electron donors in the ground state, act as electron donors in photoinduced processes when they are coupled with fullerenes in molecular dyads and triads.^{4–6}

In our previous work, we also showed that 2-pyrazolino[60]-fullerenes⁷ are excellent acceptors, since they are characterized

by less negative reduction potentials compared to other fullerene derivatives such as pyrrolidino[60]fullerenes or Diels–Alder adducts.⁸ The small HOMO–LUMO energy gaps in the corresponding donor–acceptor assemblies,⁹ consequently, lead to an efficient behaviour as constituents of plastic solar cells.¹⁰ However, donor–acceptor systems formed by TTF and a 2-pyrazolino[60]fullerene have not been reported until now, despite the evident interest in combining these moieties. In this study, we now wish to report the facile preparation of an important intermediate, a *bis*-anilino derivative in the pyrazolino[60]fullerene (PzC₆₀) series, and the electrochemical and photophysical behaviour of a new TTF–(spacer)–PzC₆₀–(spacer)–TTF triad, as shown in Chart 1. For the purposes of comparison, a reference compound, possessing two heptyl chains instead of both TTF moieties, was also prepared. In order to confirm the photoinduced charge separation and subsequent charge recombination processes, we employed time-resolved fluorescence measurements in a picosecond timescale and transient absorption measurements in a nanosecond timescale in the visible and near-IR regions.

Results and discussion

Synthesis and characterization

Among TTF derivatives, it is well-known that tetrathio-TTF units are excellent donors.⁵ The synthesis of such TTF units is summarized in Scheme 1, in which tetrathio-TTF derivative **3**, bearing a carboxylic acid group, was prepared from **1** in two steps. After hydrolysis of TTF-methyl ester **2**, obtained by

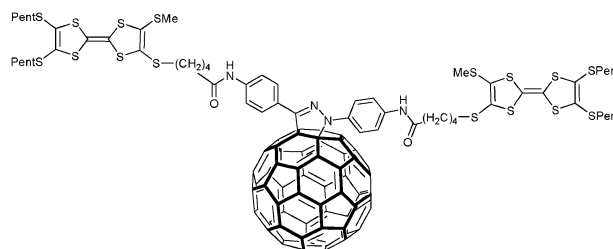


Chart 1 TTF–(spacer)–PzC₆₀–(spacer)–TTF (7).

^a Facultad de Ciencias del Medio Ambiente, Universidad de Castilla-La Mancha, 45071 Toledo, Spain. E-mail:

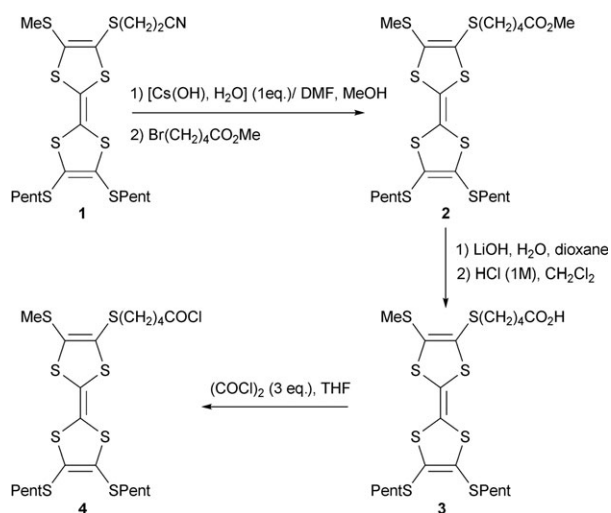
Fernando.Lpuente@uclm.es; Fax: +34 902 204 130

^b Chimie, Ingénierie Moléculaire et Matériaux d'Angers, UMR CNRS 6200, Université d'Angers, 2 Bd. Lavoisier, 49045 Angers Cedex 01, France. E-mail: cousseau@sciences.univ-angers.fr; Fax: +33 02 41 73 53 75

^c Departamento de Química Orgánica, ICMA, Universidad de Zaragoza-CSIC, E-50009 Zaragoza, Spain

^d IMRAM, Tohoku University, Katahira, Aoba-ku, 980-8577 Sendai, Japan. E-mail: ito@tagen.tohoku.ac.jp; Fax: +81 22-217-5608

† Electronic supplementary information (ESI) available: Characterization details and data of the computational studies for the new compounds described in the paper. See DOI: 10.1039/b613466a.



Scheme 1 Synthesis of TTF derivatives.

following Becher's strategy,¹¹ *via* reaction with lithium hydroxide in a water–dioxane medium according to known procedures,¹² the expected TTF-acid **3** was obtained in 95% yield. Finally, the TTF-acid chloride **4** was quantitatively prepared from compound **3** *via* the usual method using oxalyl chloride in CH_2Cl_2 and reacted *in situ*.

Compound **6** (Scheme 2) was prepared in 72% yield from *bis*-nitrophenylpyrazolino[60]fullerene (**5**),¹³ by reduction of the two nitro functions according to a previously reported procedure.¹⁴ A large excess of tin powder was added to a solution of fullerene derivative **5**, followed by several portions of concentrated aq. HCl (37%) over 25 min. The reaction was stirred for 72 h at room temperature. The mixture was hydrolyzed and the resulting solid purified by column chromatography on silica gel using CH_2Cl_2 as solvent. Thus, *bis*-anilino-2-pyrazolino[60]fullerene (**6**), which is a key and accessible building block for the preparation of C_{60} -based triads, was easily obtained. Both amino groups offer further possibilities for functionalization by simple condensation reactions, and thus give rise to new derivatives useful for applications in medicinal chemistry and material science.¹⁵

Finally, triad **7** was obtained in 90% yield (Scheme 2) by condensation of TTF-acid chloride **4** (synthesized *in situ* by treatment of TTF-acid **3** with an excess of oxalyl chloride over

2 h in refluxing CH_2Cl_2) with fullerene **6** in CH_2Cl_2 at room temperature for 10 min.

Following the same procedure, the reaction of *n*-caprylic acid chloride with pyrazolino[60]fullerene **6** in CH_2Cl_2 leads to the formation of model compound **8** in 95% yield (Scheme 2). Triads **7** and **8** were purified by several centrifugations with acetone and methanol, and their purities were checked by HPLC (see the ESI†).

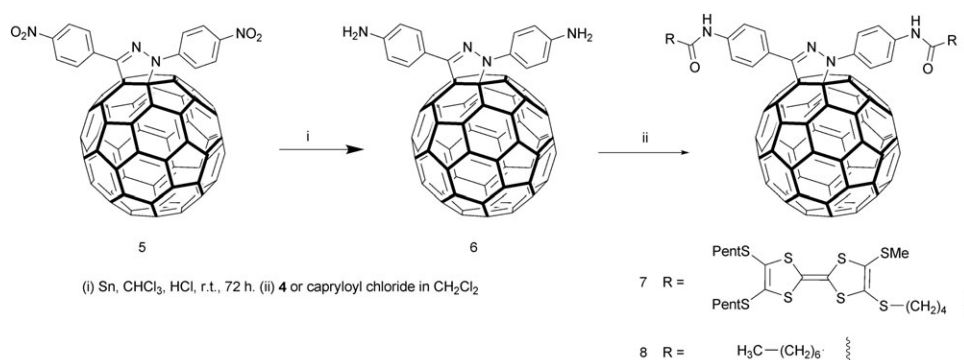
The structures of TTF derivatives **1–3** and fullerene systems **5–8** were confirmed by their analytical and spectroscopic data, such as ^1H and ^{13}C NMR, however the poor solubility of compound **8** did not allow the corresponding ^{13}C NMR spectrum to be obtained. The ^1H NMR spectrum of **7** in CD_2Cl_2 displayed only the expected signals of the *bis*-anilino-pyrazolino[60]fullerene core, the two *para*-substituted phenyl systems exhibiting signals at 8.2 and 7.8 ppm, and at 7.6 and 7.5 ppm, respectively. The protons of the two amide NH groups provided signals at 7.3 and 7.2 ppm, while the signals corresponding to the protons of the TTF unit appeared between 2.8 and 0.8 ppm. The ^{13}C NMR spectrum of **7** was in full agreement with the proposed structure, the signals from the TTF moiety, as well as from the fullerene system for the most part, appearing between 148.0 and 137.0 ppm.

The ^1H NMR spectrum of **8** showed the corresponding signals of the *para*-substituted phenyl moiety and the amide NH group between 8.2 and 7.1 ppm, and the protons of the alkyl chain between 2.45 and 2.30 ppm.

The structures of compounds **3** and **6–8** were also confirmed by MALDI-TOF mass spectra, which show the expected molecular ions at $m/z = 586.4$ (**3**), 944.0 (**6**), 2081.0 (**7**) and 1198.7 (**8**).

Molecular orbital calculations

The flexibility of the spacers in **7** leads to a high number of conformations displaying similar energy. A conformational search was conducted by using simulated annealing with the MM+ force field, as implemented in Hyperchem, leading to a minimum energy that corresponds to a bent conformation, with the center of the TTF moieties placed at 7.0 and 7.2 Å, respectively, from the center of the C_{60} core (**a** in Fig. 1). Conformations with the two TTF moieties separated away from the C_{60} (**c** in Fig. 1) are *ca.* 22–24 kcal mol⁻¹ less stable than this geometry, while those conformations with one TTF close to the fullerene spheroid and the other one separated



Scheme 2 Synthesis of triad **7** and model compound **8**.

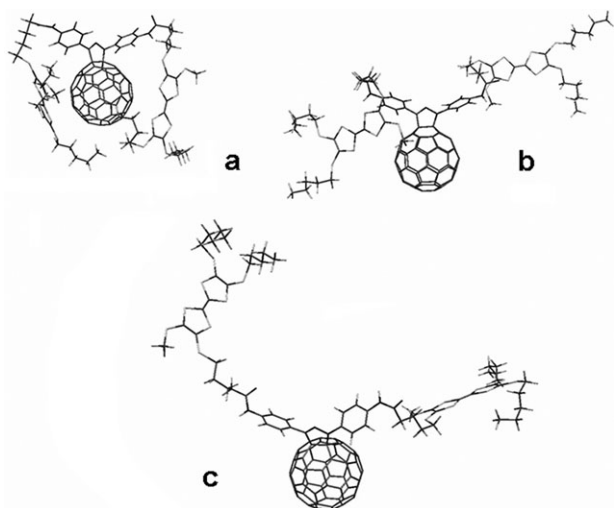


Fig. 1 Representative conformers of 7.

from it (b in Fig. 1) are *ca.* 12 kcal mol⁻¹ above the more stable conformation. However, we cannot trust these differences in energy since the MM + force field yields a poor description of the π - π interactions that are responsible for the preference for the folded conformer.

Electrochemical studies

The electrochemical properties of triad 7, and the precursors TTF-acid 3 and C₆₀, were studied by cyclic voltammetry (CV) and Osteryoung square-wave voltammetry (OSWV) in a mixture of *ortho*-dichlorobenzene (*o*-DCB)/acetonitrile (4 : 1) as the solvent (Table 1 and Fig. 2). Triad 7 gave rise to three reversible, one-electron reduction waves (see CV in the ESI[†]), which were attributed to the fullerene moiety.¹⁶ The first reduction peak of triad 7 was shifted negatively by 50 mV compared to that of the pristine C₆₀. Such an appreciable shift of the reduction wave from that of C₆₀ is similar to that observed for 6.

In the cyclic voltammograms (see the ESI[†]), two reversible oxidation waves were observed for 3 and 7 in the 0.05–0.11 and 0.33–0.39 V regions, which correspond to the formation of the radical cation and the dication species of the TTF moiety.¹⁷ Comparing these values with the observed E_{ox}^1 values of 3, a weak electronic interaction with the C₆₀ sphere in the ground state of 7 may be anticipated, although the E_{red}^1 may also be affected by the Pz moiety in addition to this interaction. The two oxidation potentials observed for *bis*-amino fullerene derivative 6 are attributed to the two different NH₂

Table 1 OSWV data for 6, triad 7, parent TTF-acid 3 and C₆₀^a

Compound	E_{ox}^1/V	E_{ox}^2/V	$E_{\text{red}}^1/\text{V}$	$E_{\text{red}}^2/\text{V}$	$E_{\text{red}}^3/\text{V}$
C ₆₀			-0.96	-1.37	-1.84
6	0.12	0.36	-0.99	-1.39	-1.99
3	0.11	0.39			
7	0.05	0.33	-1.01	-1.39	-1.90

^a *n*-Bu₄NClO₄ (0.1 M); glassy carbon electrode as the working electrode, scan rate, 100 mV s⁻¹, in *o*-DCB/acetonitrile (4 : 1).

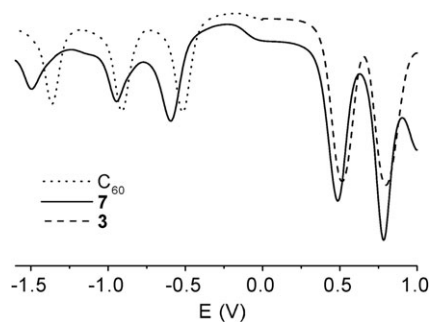


Fig. 2 OSWV data for triad 7, parent TTF 3 and C₆₀

groups according to the electrochemical studies undertaken on analogous systems.¹⁴

Steady-state UV-vis spectra

The absorption spectrum of 7 (Fig. 3) was essentially the same as the added spectra of precursors 3 and 6. However, a weak absorption at a wavelength between 400–500 nm can be ascribed to an extra absorption from the components, suggesting that there is a possible electronic interaction between them in the ground state. As discussed later, triad 7 was repetitively subject to laser light; the absorption spectrum measured after laser photolysis with 400 and 532 nm light was almost the same as before the laser irradiation, indicating that triad 7 was considerably photostable.

Steady-state fluorescence spectra

As a preliminary investigation on the photophysical properties of triad 7, steady-state fluorescence spectra of fullerene derivatives 5–8 were measured in toluene and CH₂Cl₂ at room temperature. No significant differences were observed between these two solvents (Fig. 4).

Under 430 nm excitation, which can generate the excited state (S₁) of [60]fullerene (¹C₆₀*), a broad fluorescence derived from the [60]fullerene moiety was observed around 700 nm,¹⁸ exclusively in the cases of *bis*-nitrophenyl 5 and *bis*-heptylamide 8. On the contrary, the fluorescence was almost completely quenched in *bis*-TTF derivative 7 and *bis*-anilino-2-pyrazolino[60]fullerene 6, even in toluene solvent. Due to

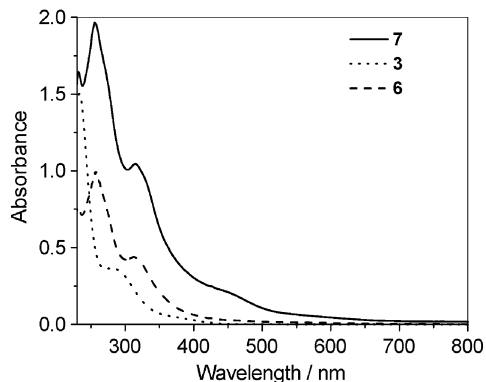


Fig. 3 Steady-state absorption of 7 (0.1 mM), 3 (0.1 mM) and 6 (0.1 mM) in CH₂Cl₂.

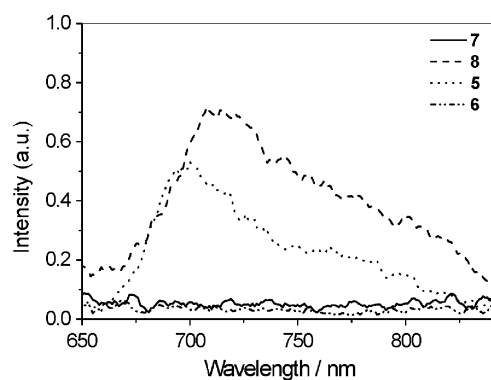


Fig. 4 Fluorescence spectra of compounds **5–8** using toluene solutions with the same absorption intensity at $\lambda_{\text{exc}} = 430$ nm.

fluorescence quenching of C_{60} , only a charge separation process can be considered, since the energy level of ${}^1\text{C}_{60}^*$ is the lowest among the constituents, such as the TTF and Pz moiety. In order to discard possible charge separation processes from the nitrogen lone pair of the pyrazoline to the C_{60} cage, as was observed previously in some 2-pyrazolino[60]fullerenes with donor units linked to the C atom of the pyrazoline ring,¹⁹ we measured the fluorescence spectrum of **7** in the presence of an equimolar amount of trifluoroacetic acid. In this case, no recovery of the fluorescence was observed, showing that the nitrogen lone pair is not responsible for the fluorescence quenching. The quenching of fluorescence in triad **7**, not observed in the analogous alkyl derivative **8**, can be ascribed to a through-space electron transfer from the TTF units to the fullerene moiety, in agreement with theoretical calculations, which show that triad **7** can adopt a folded conformation (see Fig. 1). On the other hand, an efficient fluorescence recovery was observed in the spectrum of **6** with the addition of TFA, indicating that quenching of the fluorescence in **6** is due to a photoinduced electron transfer from the aniline moiety to the C_{60} cage; the short distance between the two anilino groups and the C_{60} spheroid makes the charge separation *via* ${}^1\text{C}_{60}^*$ easy.

Time-resolved fluorescence measurements

The time-resolved fluorescence spectra of **7** in the time region from 50–1000 ps, measured by a streak camera, which has a high sensitivity in this wavelength region, are shown in Fig. 5(a).

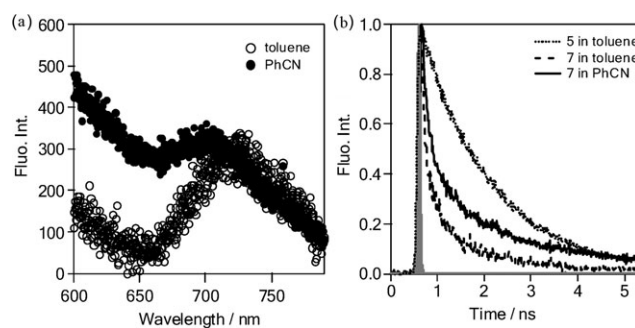


Fig. 5 (a) Fluorescence spectra of **7** in the 50–1000 ps region, measured with a streak scope detector (intensity is normalized at 700 nm), and (b) fluorescence time profiles of triad **7** in the 700–750 nm region, comparing reference **5** in toluene and PhCN; $\lambda_{\text{ex}} = 400$ nm.

The fluorescence peak near to 700 nm can be observed, which may be invisible in the steady-state fluorescence spectra in Fig. 4. For the charge separation process of triad **7**, the fluorescence lifetimes were measured in toluene and PhCN, as shown in Fig. 5(b), in which the fluorescence time profiles in the 700–750 nm region of the ${}^1\text{C}_{60}^*$ moiety of triad **7** showed the rapid decay of the C_{60} fluorescence compared to the pristine C_{60} and PzC_{60} (time profile of reference compound **5** (τ_{f0}) = 1400 ns).

These time profiles were curve-fitted with a dual exponential function, from which a major short lifetime and a minor longer lifetime were evaluated. The major short lifetimes (τ_f) are summarized in Table 2. From the τ_f values, the rate constants (k_{CS}^{S}) and quantum yields ($\Phi_{\text{CS}}^{\text{S}}$) of the charge separation *via* the ${}^1\text{C}_{60}^*$ moiety were calculated, as listed in Table 2.

The k_{CS}^{S} and $\Phi_{\text{CS}}^{\text{S}}$ values are in the range $3.8\text{--}10 \times 10^9 \text{ s}^{-1}$ and $0.85\text{--}0.94$, respectively, which supports the highly effective charge separation of triad **7** *via* the ${}^1\text{C}_{60}^*$ moiety, probably because the charge separation process belongs near to the top region of the Marcus parabola. Since the k_{CS}^{S} and $\Phi_{\text{CS}}^{\text{S}}$ values decrease with increasing the solvent polarity, the sliding down of the charge separation process from the top to the inverted region was suggested in the highly polar solvents.

In the case of a previously reported C_{60} analogue [$\text{C}_{60}(\text{TTF})_2$] (**9**) (Chart 2), in which two identical tetrathio-substituted TTF moieties are connected to C_{60} through the same flexible linkers, an appreciable shortening of the fluorescence lifetimes was not observed in non-polar and less-polar solvents.^{5b} It was deduced that the charge separation process

Table 2 Fluorescence lifetime (τ_f , at 700–750 nm), rate constant (k_{CS}^{S}), quantum yield ($\Phi_{\text{CS}}^{\text{S}}$) and free energy change ($\Delta G_{\text{CS}}^{\text{S}}$) for charge separation *via* ${}^1\text{C}_{60}^*$, rate constant (k_{CR}), radical ion pair lifetime (τ_{RIP}) and free energy change (ΔG_{CR}), for the charge recombination of triad **7**^a

Solvent	ϵ	τ_f/ps (fraction (%))	$k_{\text{CS}}^{\text{S}}/\text{s}^{-1}$	$\Phi_{\text{CS}}^{\text{S}}$	$\Delta G_{\text{CS}}^{\text{S}}/\text{eV}$	$k_{\text{CR}}/\text{s}^{-1}$	$\tau_{\text{RIP}}/\text{ns}$	$\Delta G_{\text{CR}}/\text{eV}$
Toluene	2.38	90 (90)	1.0×10^{10}	0.94	−0.10	1.6×10^7	60	−1.60
THF	7.58	120 (92)	7.8×10^9	0.92	−0.54	7.7×10^6	130	−1.16
CH_2Cl_2	8.93	110 (89)	8.7×10^9	0.93	−0.57	4.4×10^6	230	−1.13
PhCN	25.20	150 (75)	6.0×10^9	0.90	−0.71	1.8×10^7	60	−0.69
DMF	36.71	220 (60)	3.8×10^9	0.85	−0.75	7.4×10^6	140	−0.65

^a $k_{\text{CS}}^{\text{S}} = (1/\tau_f) - (1/\tau_{f0})$; $\Phi_{\text{CS}}^{\text{S}} = [(1/\tau_f) - (1/\tau_{f0})]/(1/\tau_{f0})$; ϵ = solvent dielectric constant; $\Delta G_{\text{CS}}^{\text{S}}$ and ΔG_{CR} were calculated by the same method previously described, assuming center-to-center distance (R_{CC}) = 7 \AA .^{5b}

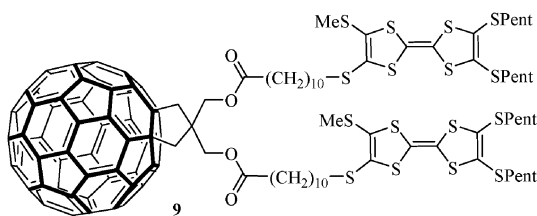


Chart 2 $[C_{60}(TTF)_2]$ (**9**).

took place *via* the $^3C_{60}^*$ moiety in these solvents.^{5b} On the other hand, TTF-(spacer)-PzC₆₀-(spacer)-TTF (**7**), in the present study, showed faster fluorescence quenching rates in non-polar and less-polar solvents rather than in highly polar solvents. Therefore, the charge separation process of triad **7** takes place predominantly *via* the $^1C_{60}^*$ moiety, not *via* the $^3C_{60}^*$ moiety.

Furthermore, the slow decay component (*ca.* 1.3 ns) exhibited a low contribution (10–40%) that follows an intersystem crossing (ISC), leading to the $^3C_{60}^*$ moiety, even in polar solvents.

Transient absorption spectra

In order to confirm the event of a charge separated state, transient absorption spectra were measured in various solvents. One example in CH₂Cl₂ is shown in Fig. 6, in which broad absorption bands are observed in the wide 550–1200 nm wavelength region.

These absorption spectra are quite similar to the previously observed transient spectra for the $[C_{60}(TTF)_2]$ triad **9**, possessing the same tetrathio-substituted TTFs.^{5b} The absorption around 1000 nm can be attributed to the radical anion of the fullerene moiety, whereas the broad band in the 600–900 nm region can be attributed to the cation radical of tetrathio-substituted TTF, which decayed at almost the same rate.^{5b} Therefore, the generation of the radical ion pair (TTF)^{•+}-(spacer)-Pz(C₆₀)^{•-}-(spacer)-TTF is suggested, in which an electron is located on the C₆₀ moiety and a hole is located on one of the tetrathio-substituted TTF moieties.

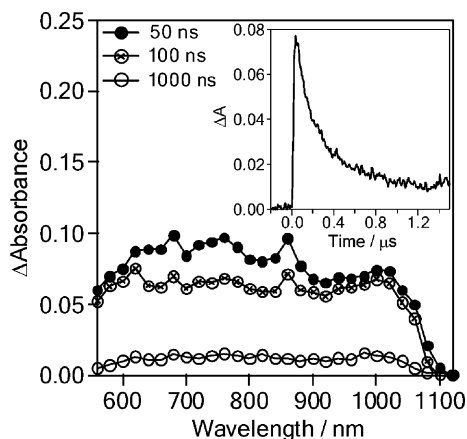


Fig. 6 Transient absorption spectra of triad **7** observed with 532 nm laser light excitation in Ar-saturated CH₂Cl₂. Inset: Time profile at 1020 nm.

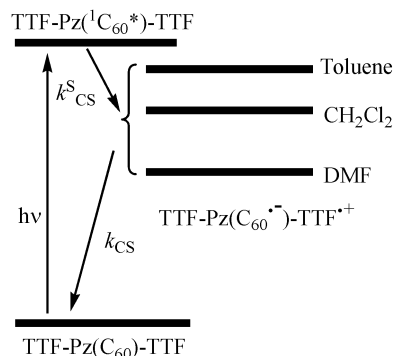


Fig. 7 Schematic energy diagram: TTF-(spacer)-PzC₆₀-(spacer)-TTF is abbreviated as TTF-Pz(C₆₀)-TTF.

As shown in the inset of Fig. 6, the time profile at 1020 nm, which is the same as those in the visible region, decayed with almost first-order kinetics, giving a charge-recombination rate constant (k_{CR}) = 4.4×10^6 s⁻¹ in CH₂Cl₂ at room temperature, from which the lifetime of the radical ion pair (RIP) (τ_{RIP}) was found to be 230 ns (Table 2). Moreover, relatively long τ_{RIP} values were found in THF (130 ns) and DMF (140 ns), whereas shorter τ_{RIP} values were determined in toluene (60 ns) and PhCN (60 ns). Thus, plots of τ_{RIP} values *vs.* solvent polarity ($1/\epsilon$) show a maximum, except for PhCN. This behaviour is quite different from that of $[C_{60}(TTF)_2]$ triad **9**, in which a monotonous increase of the τ_{RIP} value from 30 ns (in PhCN) to 110 ns (in toluene) was observed.^{5b} Since this order cannot be explained by the Marcus theory, some specific factors, such as preferential solvation of (TTF)^{•+}-(spacer)-Pz(C₆₀)^{•-}-(spacer)-TTF, may play important roles.

Energy diagram

From Table 2, the free energy changes of charge separation (ΔG_{CS}^S) *via* the $^1C_{60}^*$ moiety and charge recombination (ΔG_{CR}) were evaluated, as listed in Table 2 using the redox potentials from Table 1 and optimized structure from Fig. 1. From these data, the energy diagram can be schematically depicted, as shown in Fig. 7. The most prominent difference from the $[C_{60}(TTF)_2]$ triad **9** is the absence of the $^3C_{60}^*$ moiety route for the charge separation process, and consequently the absence of triplet spin character in the RIP. Thus, the observed k_{CS}^S and k_{CR} values may depend mainly on the Marcus theory for the RIP possessing a singlet spin character. Assuming the reorganization energy to be 0.5–0.7 eV,²⁰ a maximal k_{CS}^S value would be anticipated in intermediate polar solvents but a maximal k_{CR} value in highly polar solvents.

However, these observations for triad **7**, with the pyrazoline group, do not always trace the Marcus parabola. This suggests that in this particular molecule, the pyrazoline group influences both topologically and electronically the stabilization of the charge separated state and through-space electron transfer.

Conclusions

A new triad, **7**, based on a 2-pyrazolino[60]fullerene system possessing two TTF units connected with flexible long

linkages, has been synthesized and its properties compared with a model compound without TTF units, **8**.

Electrochemical studies and UV-vis spectra suggest the existence of a weak electronic interaction in the ground state between the fullerene cage and the TTF units. In the excited state, triad **7** showed an efficient quenching of the fluorescence of the C₆₀ moiety with respect to the emission observed for alkyl derivative **8**. This fluorescence quenching can be ascribed to a through-space electron transfer from the TTF units to the C₆₀ moiety.

Laser spectroscopy studies have demonstrated that a highly effective charge separation of triad **7** in polar and non-polar solvents (with quantum yields between 0.85 and 0.94) takes place *via* a ¹C₆₀* moiety. The longest lifetime of the charge separated state was found to be 230 ns in CH₂Cl₂ solvent, clearly longer than other [C₆₀(TTF)₂] derivatives previously observed. These results suggest that the pyrazoline ring participates in the photoinduced electron transfer process. Further investigations are now in progress.

Experimental section

All cycloaddition reactions were performed under argon. C₆₀ was purchased from MER Corporation (Tucson, AZ). TLC using Merck silica gel 60-F254 was used to monitor cycloaddition reactions. ¹H NMR and ¹³C NMR spectra were recorded on Varian Mercury 200 and Varian Inova 500 spectrometers. UV-vis absorption spectra were obtained on a Shimadzu spectrophotometer. Steady-state fluorescence spectra were measured on a Varian Cary spectrofluorophotometer. FT-IR spectra were recorded on a Nicolet Impact 410 spectrophotometer using KBr disks. MALDI-TOF mass spectra were obtained on a Voyager-STR spectrometer. Cyclic voltammetry measurements were carried out on an Autolab PGSTAT 30 potentiostat using a BAS MF-2062, Ag/0.01 mol L⁻¹ AgNO₃ as a reference electrode, an auxiliary electrode consisting of a Pt wire, a Metrohm 6.1247.000 conventional glassy carbon electrode (GCE, 3 mm o.d.) as a working electrode directly immersed into the solution containing 0.1 mol L⁻¹ TBAP as an electrolyte in *o*-DCB/acetonitrile (4 : 1). A 10 mL electrochemical cell from BAS, model VC-2, was also used. The reference potential was shifted by 290 mV towards a more negative potential compared to the Ag/AgCl scale. *E*_{1/2} values were taken as the average of the anodic and cathodic peak potentials. Scan rate 100 mV s⁻¹. The ps time-resolved fluorescence spectra were measured using an argon-ion pumped Ti:sapphire laser (Tsunami; pulse width = 2 ps) and a streak scope (Hamamatsu Photonics; response time = 10 ps). Details of the experimental setup are described elsewhere.²¹ Nanosecond transient absorption spectra in the NIR region were measured by means of laser-flash photolysis; 532 nm light from a Nd:YAG laser (pulse width = 6 ns) was used as the exciting source and a Ge-avalanche-photodiode module was used for detecting the monitoring light from a pulsed Xe lamp, as described in our previous report.²¹ Molecular Mechanics calculations were performed using the HYPERCHEM 7.5 package.

6,7-Bis(pentylsulfanyl)-2-methoxycarbonylbutylsulfanyl)-3-methylsulfanylTTF (2). [CsOH, H₂O] (0.406 g, 2.42 mmol)

dissolved in the minimum amount of dry ethanol was added, under nitrogen, to a solution of compound **1** (870 mg, 1.61 mmol) in 40 mL dry DMF. After 30 min stirring, methyl 5-bromopentanoate (0.46 mL, 3.22 mmol) was added and the reaction mixture stirred at room temperature for a further 4 h. After the evaporation of DMF, the residue was dissolved in CH₂Cl₂ and this organic phase washed with water then dried over magnesium sulfate. After evaporation of the solvent, the crude solid was purified by column chromatography (silica gel, CH₂Cl₂/hexane 2 : 9), leading to pure compound **2** (90% yield). ¹H NMR (500 MHz, CDCl₃/ppm) 3.66 (s, 3 H), 2.79–2.83 (m, 6 H), 2.42 (s, 3 H), 2.34 (t, 2 H, *J* = 7.3 Hz), 1.75–1.77 (m, 2 H), 1.61–1.67 (m, 6 H), 1.31–1.40 (m, 8 H) and 0.90 (t, 6 H, *J* = 7.2 Hz).

2-Carboxybutylsulfanyl-3-methylsulfanyl-6,7-dipentylsulfanyl-TTF (3). Compound **2** (0.87 g, 1.45 mmol) was dissolved, under nitrogen, in 110 mL dioxane in a 1 L three-necked round-bottomed flask. Then, [LiOH, H₂O] (0.61 g, 14.5 mmol) dissolved in 55 mL water was added dropwise at room temperature. After 24 h stirring, 220 mL CH₂Cl₂ and 65 mL aq. 1 M HCl were added and the resulting mixture kept under stirring for 24 h. The organic phase was separated, washed with water until neutral and then dried over anhydrous magnesium sulfate. After evaporation of the solvent, the residue was purified by column chromatography (silica gel, CH₂Cl₂ then ethyl acetate), giving rise to pure compound **3** (95% yield). ¹H NMR (500 MHz, CDCl₃/ppm) 2.79–2.84 (m, 6 H), 2.41 (s, 3 H), 2.30 (t, 2 H, *J* = 7.0 Hz), 1.60–1.75 (m, 8 H), 1.30–1.40 (m, 8 H) and 0.9 (t, 6 H, *J* = 7.2 Hz); ¹³C NMR (50 MHz, CD₂Cl₂ + Et₃N/ppm)²² 178.8, 129.3, 128.1, 127.8, 126.4, 110.6, 110.3, 36.6, 36.5, 36.4, 30.9, 29.9, 29.7, 25.3, 22.4, 19.3 and 14.1; MALDI-TOF *m/z* 586.4 (M⁺).

3'-(4-Aminophenyl)-1'-(4-aminophenyl)pyrazolino [4',5';1,2][60] fullerene (6). Tin powder (1.5 g) was added to a solution of **5** (50 mg, 0.05 mmol) in chloroform (75 mL). Concentrated HCl (25 mL) was added in 5 portions over 25 min, then 0.5 g of tin powder and a further 5 mL portion of hydrochloric acid were added. The mixture was stirred at room temperature for 72 h then neutralized with a concentrated sodium hydroxide solution. The aqueous phase was extracted with CH₂Cl₂. The organic layers were then dried over MgSO₄ and evaporated. The crude solid was purified by column chromatography (silica gel, CH₂Cl₂) affording **6** in 72% yield (34 mg, 0.04 mmol). FT-IR (KBr) ν /cm⁻¹ 3441, 3375, 1616, 1507, 1183, 1107, 822 and 520; ¹H NMR (400 MHz, CDCl₃/ppm) 8.10 (d, 2 H, *J* = 8.8 Hz), 7.60 (d, 2 H, *J* = 8.8 Hz), 6.70 (d, 4 H, *J* = 8.8 Hz), 3.90 (bs, 2 H) and 3.76 (bs, 2 H); ¹³C NMR (100 MHz, CDCl₃/ppm) 147.2, 147.0, 146.6, 146.5, 146.2, 146.1, 145.9, 145.7, 145.6, 145.5, 145.2, 145.1, 130.6, 130.1, 128.6, 126.7, 122.5, 122.3, 115.5 and 114.7; MALDI-TOF *m/z* 944.0 (M⁺ – H).

1',3'-Bis(4-(2-butylsulfanyl-3-methylsulfanyl-6,7-dipentylsulfanyl)tetrahydrofulvalenoyl)phenylamide)-2-pyrazoline[4',5':1,2][60] fullerene (7). TTF-acid **3** (74 mg, 0.13 mmol) was refluxed in CH₂Cl₂ (25 mL) in the presence of a large excess of oxalyl chloride over 2 h. The solvent and excess of reagent were then removed under vacuum. The resulting oil was dissolved in 5

mL dry CH₂Cl₂, and added to a CH₂Cl₂ solution (50 mL) of **6** (20 mg, 0.02 mmol) and pyridine (15 µL). The mixture was stirred at room temperature under argon for 10 min. The solvent was evaporated, and the resulting solid purified by centrifugation with acetone and then methanol to give **7** in 90% yield (39 mg, 0.02 mmol). FT-IR (KBr) ν/cm^{-1} 2917, 2843, 1666, 1589, 1503, 1454, 1397, 1307, 1249, 1180, 1102, 841, 714 and 526; ¹H NMR (400 MHz, CD₂Cl₂/ppm) 8.16 (d, 2 H, *J* = 6.4 Hz), 7.77 (d, 2 H, *J* = 6.4 Hz), 7.58 (d, 2 H, *J* = 7 Hz), 7.54 (d, 2 H, *J* = 7 Hz), 7.30 (s, 1 H), 7.21 (s, 1 H), 2.78 (t, 4 H), 2.73 (t, 8 H), 2.34 (s, 3 H), 2.33 (s, 3 H), 2.30 (t, 4 H), 1.80–1.15 (m, 32 H) and 0.88–0.80 (m, 12 H); ¹³C NMR (100 MHz, CD₂Cl₂/ppm) 147.9, 147.5, 146.7, 146.6, 146.5, 146.3, 146.3, 146.2, 146.1, 145.7, 145.5, 144.6, 143.2, 142.7, 142.6, 142.5, 141.4, 140.6, 140.1, 136.8, 136.6, 130.7, 129.9, 124.9, 120.6, 119.7, 38.4, 37.3, 36.8, 36.4, 36.4, 32.5, 31.5, 31.3, 30.3, 30.0, 29.7, 29.6, 24.7, 24.6, 22.9, 19.5 and 14.5; MALDI-TOF *m/z* 2081.0 (M⁺ – H).

1',3'-Bis(4-(heptanoyl)-phenylamide)-2-pyrazoline[4',5':1,2]@60 fullerene (8). *n*-Caprylic acid (22 mg, 0.16 mmol) was refluxed in CH₂Cl₂ (20 mL) in the presence of a large excess of oxalyl chloride for 2 h. The solvent and excess reagent were then removed under vacuum. The resulting oil was dissolved in 5 mL dry CH₂Cl₂, and then added to a CH₂Cl₂ solution of **6** (15 mg, 0.02 mmol) and pyridine (15 µL). The mixture was stirred at room temperature under argon for 10 min. The solvent was then evaporated, and the resulting solid purified by centrifugation with acetone and then methanol to give **8** in 95% yield (18 mg, 0.02 mmol). FT-IR (KBr) ν/cm^{-1} 2917, 2843, 1666, 1589, 1503, 1454, 1397, 1307, 1249, 1180, 1102, 841, 714 and 526; ¹H NMR (200 MHz, CDCl₃/ppm) 8.23 (d, 2 H, *J* = 8.6 Hz), 7.85 (d, 2 H, *J* = 8.6 Hz), 7.66 (d, 2 H, *J* = 8.4 Hz), 7.61 (d, 2 H, *J* = 8.6 Hz), 7.20 (s, 1 H), 7.13 (s, 1 H), 2.45–2.30 (m, 4 H), 1.80–1.20 (m, 20 H) and 0.89 (t, 6 H); MALDI-TOF *m/z* 1198.7 (M⁺).

Acknowledgements

Financial support for this work was provided by the MEC of Spain and FEDER funds (projects CTQ2004-00364/BQU, BQU2002-00219), the Junta de Comunidades de Castilla-La Mancha (project PAI-05-068). F. O. gives thanks for a grant from the EU (RTN contract “FAMOUS”, HPRN-CT-2002-00171). The CNRS is also gratefully acknowledged for financial support, as well as Ministère de la Recherche (France) for a PhD grant to S. C. We also thank to Dr. Z. Gan for his help with the photophysical measurements.

References

- (a) D. Gust, T. A. Moore and A. L. Moore, *Acc. Chem. Res.*, 2001, **34**, 40; (b) K. G. Thomas, M. V. George and P. V. Kamat, *Helv. Chim. Acta*, 2005, **88**, 1291.
- (a) C. J. Brabec, N. S. Saricifti and J. C. Hummelen, *Adv. Funct. Mater.*, 2001, **11**, 15; (b) H. Imahori and S. Fukuzumi, *Adv. Funct. Mater.*, 2004, **14**, 525.

- P. J. Bracher and D. I. Schuster, *Electron Transfer in Functionalized Fullerenes*, in *Fullerenes: From Synthesis to Optoelectronic Properties*, ed. D. M. Guldi and N. Martin, Kluwer Academic Publishers, Dordrecht, 2002, ch. 6, pp. 163–212.
- M. Bendikov, F. Wudl and D. Perepichka, *Chem. Rev.*, 2004, **104**, 4891 and references therein.
- (a) E. Allard, J. Cousseau, J. Ordúna, J. Garin, H. Luo, Y. Araki and O. Ito, *Phys. Chem. Chem. Phys.*, 2002, **4**, 5944; (b) S. Chopin, Z. Gan, J. Cousseau, Y. Araki and O. Ito, *J. Mater. Chem.*, 2005, **15**, 2288; (c) M. Di Valentin, A. Bisol, G. Agostini, P. A. Liddell, G. Kodis, A. L. Moore, T. A. Moore, D. Gust and D. Carbonera, *J. Phys. Chem. B*, 2005, **109**, 14401.
- (a) D. M. Guldi, *Chem. Commun.*, 2000, 321; (b) N. Martín, L. Sánchez, C. Seoane, R. Andreu, J. Garin and J. Orduna, *Tetrahedron Lett.*, 1996, **37**, 5979; (c) N. Martín, L. Sánchez, M. A. Herranz and D. M. Guldi, *J. Phys. Chem. A*, 2000, **104**, 4648; (d) D. M. Guldi, S. González, N. Martín, A. Antón, J. Garin and J. Orduna, *J. Org. Chem.*, 2000, **65**, 1978; (e) J. L. Segura, E. M. Priego and N. Martín, *Tetrahedron Lett.*, 2000, **41**, 7737; (f) A. G. Burly, A. G. Avent, O. B. Boltina, V. G. Ilya, D. M. Guldi, M. Marraccacio, F. Paolucci, D. Paolucci and R. Taylor, *Chem. Commun.*, 2003, 148.
- E. Espildora, J. L. Delgado, P. de la Cruz, A. de la Hoz, V. López-Arza and F. Langa, *Tetrahedron*, 2002, **58**, 5821.
- (a) F. Langa, P. de la Cruz, E. Espildora, A. de la Hoz, J. L. Bourdelande, L. Sánchez and N. Martín, *J. Org. Chem.*, 2001, **66**, 5033; (b) F. Langa, M. J. Gomez-Escalonilla, J. M. Rueff, T. M. Figueira-Duarte, J. F. Nierengarten, V. Palermo, P. Samorí, Y. Río, G. Accorsi and N. Armaroli, *Chem.–Eur. J.*, 2005, **11**, 4405.
- D. F. Perepichka and M. R. Bryce, *Angew. Chem., Int. Ed.*, 2005, **44**, 2.
- (a) X. Wang, E. Perzon, J. L. Delgado, P. de la Cruz, F. Zhang, F. Langa, M. R. Andersson and O. Inganäs, *Appl. Phys. Lett.*, 2004, **85**, 5081; (b) X. Wang, E. Perzon, F. Oswald, F. Langa, S. Admassie, M. R. Andersson and O. Inganäs, *Adv. Funct. Mater.*, 2005, **15**, 1665.
- J. Becher, J. Lau, P. Leriche, P. Mørk and N. Svenstrup, *J. Chem. Soc., Chem. Commun.*, 1994, 2715.
- R. P. Parg, J. D. Kilburn, M. C. Petty, C. Pearson and T. G. Ryan, *Synthesis*, 1994, 613.
- J. L. Delgado, P. de la Cruz, V. Lopez-Arza, F. Langa, Z. Gan, Y. Araki and O. Ito, *Bull. Chem. Soc. Jpn.*, 2005, **78**, 1500.
- J. L. Delgado, P. de la Cruz, V. López-Arza and F. Langa, *Tetrahedron Lett.*, 2004, **45**, 1651.
- K. Kordatos, T. Da Ros, S. Bosi, E. Vazquez, M. Bergamin, C. Cusan, F. Pellarini, V. Tomberli, B. Baiti, D. Pantarotto, V. Georgakilas, G. Spalluto and M. Prato, *J. Org. Chem.*, 2001, **66**, 4915.
- M. A. Herranz, C. T. Cox and L. Echegoyen, *J. Org. Chem.*, 2003, **68**, 5009.
- (a) A. J. Moore and M. R. Bryce, *J. Chem. Soc., Chem. Commun.*, 1991, 1638; (b) H. Spanggaard, J. Prehn, M. B. Nielsen, E. Levillain, M. Allain and J. Becher, *J. Am. Chem. Soc.*, 2000, **122**, 9486.
- D. M. Guldi and M. Prato, *Acc. Chem. Res.*, 2000, **33**, 695.
- N. Armaroli, G. Accorsi, J.-P. Gisselbrecht, M. Gross, V. Krasnikov, D. Tsamouras, G. Hadziioannou, M. J. Gómez-Escalonilla, F. Langa, J.-F. Eckert and J.-F. Nierengarten, *J. Mater. Chem.*, 2002, **12**, 2077.
- A. S. D. Sandanayaka, Y. Araki, O. Ito, G. R. Deviprasad, P. M. Smith, L. M. Rogers, M. E. Zandler and F. D'Souza, *Chem. Phys.*, 2006, **325**, 452.
- (a) T. Nojiri, A. Watanabe and O. Ito, *J. Phys. Chem. A*, 1998, **102**, 5215; (b) M. Fujitsuka, O. Ito, T. Yamashiro, Y. Aso and T. Otsubo, *J. Phys. Chem. A*, 2000, **104**, 4876.
- M. Giffard, P. Alonso, J. Garin, A. Gorgues, T. P. Nguyen, P. Richomme, A. Robert, J. Roncali and S. Uriel, *Adv. Mater.*, 1994, **6**, 298.